
Volume 37 Number 10
December 2010
ISSN 0735-1933
ELSEVIER
International Communications in
HEAT and MASS TRANSFER
Editor-in-Chief
W.J. MINKOWYCZ
Editors
A.R. BALAKRISHNAN, P. CHENG, R. GREIF, C.P. GRIGOROPOULOS, E. HAHNE,
A.I. LEONTIEV, O.G. MARTYNENKO, J.W. ROSE, J. TAINE, H. YOSHIDA
Available online at
ScienceDirect
www.sciencedirect.com

International Communications in Heat and Mass Transfer 37 (2010) 1487–1495

Contents lists available at ScienceDirect

International Communications in Heat and Mass Transfer

journal homepage: www.elsevier.com/locate/ichmt

Microwave curing at an operating frequency of 2.45 GHz of Portland cement paste at early-stage using a multi-mode cavity: Experimental and numerical analysis on heat transfer characteristics ☆

Natt Makul [a,b,*], Phadungsak Rattanadecho [b,*], Dinesh K. Agrawal [c]

[a] *Faculty of Industrial Technology, Phranakhon Rajabhat University, 9 Changwattana Road, Bangkhen, Bangkok 10220, Thailand*
[b] *Research Center for Microwave Utilization in Engineering (R.C.M.E.), Department of Mechanical Engineering, Faculty of Engineering, Thammasat University, (Rangsit Campus), Khlong Luang, Prathum thani 12121, Thailand*
[c] *The Materials Research Institute, The Pennsylvania State University, University Park, PA 16802, USA*

ARTICLE INFO

Available online 12 November 2010

Keywords:
Cement paste
Dielectric
Heat transfer
Microstructure
Microwave energy

ABSTRACT

In this study, microwave curing at an operating frequency of 2.45 GHz of Portland cement paste at an early-stage using a multi-mode cavity is presented. First, the dielectric evolution of the cement paste at a water-to-cement mass ratio of 0.38 during a 24-h first-hydration period was measured. Secondly, the microstructural characteristics of the hardened cement paste after heating for 45 min in microwaves at a power of 390 W, with specific attention to the temperature rise were investigated experimentally and theoretically. The obtained results show that dielectric properties decrease rapidly during the hydration reaction and formation resuming and then proceeding with a high rate. During microwave heating, the temperature increased monotonically. The micrographs of the microwave-heat paste clearly indicate that the samples consisted of hydrated phases and pores, as well as cores of $Ca(OH)_2$ dendrite crystals, calcium silicate hydrate (C–S–H), and granular structure. The results of the temperature rise in our experiment without loss of moisture and steady heat transfer conduction, consistently agreed with the mathematical model developed for this study.

1. Introduction

Microwave energy has been widely used as an innovative material processing for various industrial dielectric materials such as paper, wood, etc. Basically, microwave radiation interacts with the materials through dielectric permittivity resulting in rapid heating. Consequently, dipole interaction and heat generation will take place within dielectric materials which are composed of polar molecules [1,2].

Can microwave energy be applied to cure cementitious materials? The answer based on theoretical considerations, is yes. Many research groups [3–8] have investigated, both experimentally and numerically, the accelerated curing of cements in microwaves in order to gain high strength [3]. However, the success has been very limited due to lack of understanding of the behavior of dielectric permittivity and heat transfer characteristics of cement-based materials. These properties are highly dependent upon temperature, free moisture content and hydration time. In particular, during the first 24 h of hydration, it is critical to determine optimum conditions for a high performance curing of the cementitious materials using microwave energy [4,5]. Therefore, this paper investigates first the dielectric permittivity of a 0.38-w/c cement paste during the initial period of hydration at a frequency of 2.45 GHz. The investigation uses a network analyzer with a reflection/transmission line technique to determine the dielectric properties of the cementitious material. Secondly, this paper also examines the microstructural and heat transfer characteristics of the cement paste after microwave exposure.

Dongxu and Xuequan's [6] application of a vacuum microwave composite to dewater concrete engineering is quite significant. They found that the optimum curing conditions were 45 min at 60 °C, which decreased the final water-to-cement ratio of concrete to about 0.38. With the help of the feedback control temperature, Leung and Pheeraphan [7–9] illustrated that the optimization process for microwave curing concrete depended on power level and soaking duration, which they determined to be 400 W and 45 min, respectively.

2. Related theories

Maxwell equations govern microwave heating of a cement paste. The electromagnetic wave interaction with materials is formulated in the following four equations:

$$\nabla x\vec{E} = -\mu\frac{\partial\vec{H}}{\partial t}, \nabla x\vec{H} = \sigma\vec{E} + \varepsilon\frac{\partial\vec{E}}{\partial t}, \nabla.\vec{H} = 0\ \nabla.\vec{E} = \frac{q}{\varepsilon} \quad (1)$$

where $\check{E}$ is the electric field intensity (V/m), $\check{H}$ is the magnetic field intensity (A/m), $\check{D}$ is the electric flux density (C/m), $\check{B}$ is the magnetic

☆ Communicated by W.J. Minkowycz.

* Corresponding authors. Tel.: +66 2564 3001–9x3153; fax: +66 2564 3010.
E-mail address: ratphadu@engr.tu.ac.th (P. Rattanadecho).

0735-1933/$ – see front matter © 2010 Elsevier Ltd. All rights reserved.
doi:10.1016/j.icheatmasstransfer.2010.09.001

flux density (Wb/m^2), t is the time, and q is the electric charge density (C/m^3).

The temperature rise of the processed cement paste under heating with microwave can be obtained by solving the heat-conduction transport equation included as a local electromagnetic heat-generation term [12]:

$$\rho C_p \frac{\partial T}{\partial t} + \nabla \times (-k \nabla T) = Q \quad (2)$$

where T is the temperature (°C), a is the thermal diffusivity (m^2/s), $\rho$is the density (kg/m^3), and$c_p$is the heat capacity at a constant pressure (J/(kg K)). The local electromagnetic heat-generation term Q depends on the electric field distribution defined as in Eq. (3) [12].

$$Q = \sigma E^2 = 2\pi f \varepsilon_0 \varepsilon_r' (\tan\delta) E^2 \quad (3)$$

where Q is the microwave energy (W/m^3), σ is the effective conductivity (S/m), f is the frequency (Hz), ε_0 is the permittivity of free space (F/m) (8.85142×10^{-12} F/m), $\varepsilon_r^{'}$ is the relative dielectric constant (dimensionless), tan δ is the loss tangent coefficient (dimensionless), and E^v is the electric field intensity (V/m).

3. Experimental procedures

Type I Portland cement was used throughout this study. The chemical composition and physical properties are listed in Table 1.

The Type I Portland cement paste used was proportioned at a w/c ratio of 0.38. The appropriate amounts of starting materials were weighed out to the nearest hundredth of a gram on a Mettler Pl 1200 balance. A Hobart mixer was used to mix the solids and liquids according to ASTM C 305 [10]. Samples were cast in the form of a cylinder with the dimensions of ϕ 70.0 mm × 40.0 mm. After mixing and molding, they were cured at room temperature by wrapping with polyethylene plastic until the delay time (time after mixing until introducing microwave energy with a multi-mode cavity) for 30 min.

In order to measure the dielectric properties of the paste, it was necessary to use a vector network analyzer (VNA, model HP 8519, Fig. 1 [11]). HP 8510 makes both reflection measurements and transmission measurements. An incident signal generated by an RF source is compared with the signal transmission through the analyzer or reflected from the wave input when passing the waveguide. The permittivity from s-parameters, were obtained by using the Nicholson–Ross–Weir (NRW) technique (Fig. 2).

The microwave system used in this study is shown in Fig. 3, that included an industrial microwave generator model S56F manufactured by Cober Electrics, Inc., Stanford Conn., USA. This model can generate microwave energy at 2.45 ± 0.05 GHz and a maximum power of 6.0 kW in a multimode chamber. The microwave apparatus does not provide a real-time monitoring of temperature changes during curing; therefore, the temperature of the sample was measured at the start and end of the curing process. In order to measure the temperature of the sample subjected to microwave energy, various positions of measurement were selected. The temperature of the top surface and the bottom surface was measured 5 times for each run; likewise, the sample was immediately fractured such that the temperature within it was also measured 5 times.

Table 1
Chemical composition and physical properties of the Portland cement used (% by mass).

SiO_2	Al_2O_3	CaO	Fe_2O_3	MgO	K_2O	Na_2O	SO_3	L.O.I
20.30	5.67	60.43	6.23	3.14	0.90	0.36	2.80	2.80
Specific gravity					3.12			
Surface area (BET method) (m^2/g)					0.85			

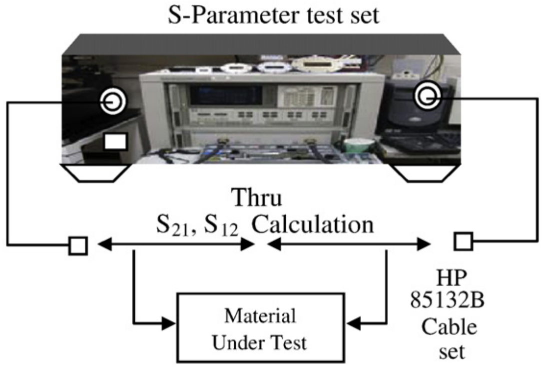

Fig. 1. Network analyzer.

4. Numerical analysis

4.1. Model outlined

In order to investigate theoretically the temperature rise during heating by microwave energy, a three-dimensional microwave-heating model is proposed. This model comprises a microwave-heating model, to show the interaction between the electromagnetic (microwave) and cement paste, a dissipation model and a heat-generation model. A detailed schematic of the simulation process is shown in Fig. 4.

4.2. Physical model

A schematic diagram of the physical model is shown in Fig. 5. The temperature of the material introduced to the incident wave is obtained by solving the conventional heat transport equation with the microwave power included as a local electromagnetic heat-generation term [13].

The materials considered were cement pastes at a w/s equal to 0.38, which consist of Portland cement Type I, water, and air. They are, therefore, homogeneous and isotropic in terms of structure. In order to analyze the process of heat transport due to microwave

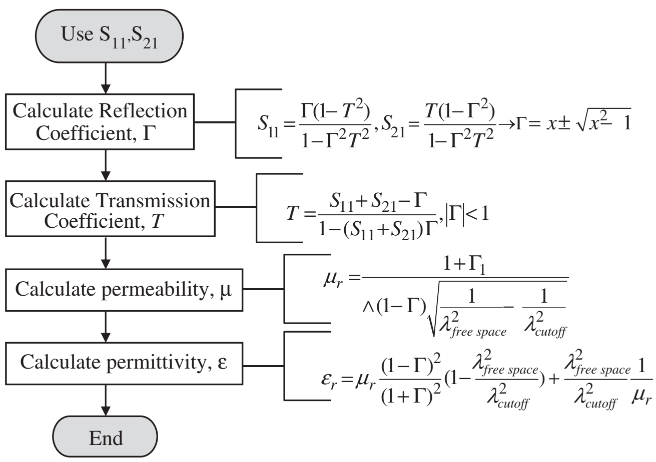

Fig. 2. Nicholson–Ross–Weir procedures.

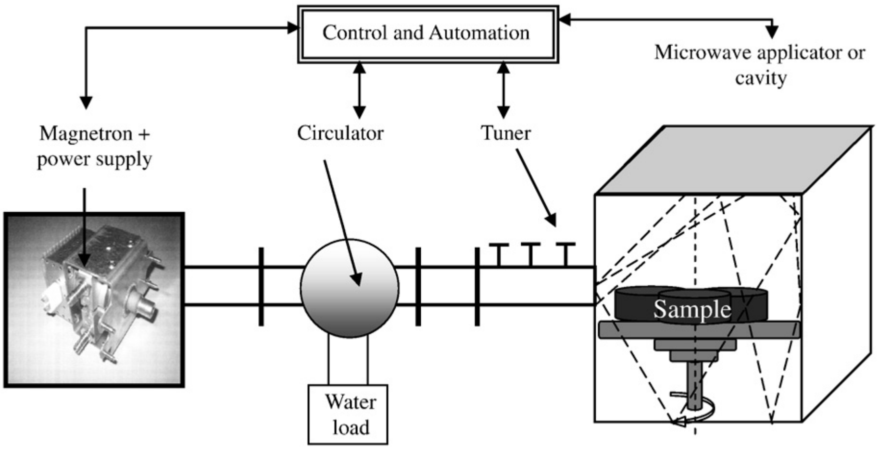

Fig. 3. Configuration of the microwave curing package.

heating of dielectric materials, the following assumptions were made:

- The local thermodynamic equilibrium among each phases is achieved.
- The absorption of microwave energy by the cavity (including air) in the multi-modes cavity is negligible.
- Three specimens of cement paste absorb with the energy equivalent during applying microwave radiation and rotating with a turning disk, resulting in a specimen is taken into account.
- No chemical reactions within the material.
- Radiation mode is negligible.
- The effect of the natural and induced convections can be neglected.

In this task, from a macro-level point of view, the pore structure within the microwave-cured paste is assumed to be uniform. Furthermore, a heating model for a homogeneous and isotropic material is used in this analysis.

4.3. Governing equations

The governing equations describing the temperature rise in the paste to be processed by microwave energy are:

(1) Electromagnetic wave:
As shown in Eq. (1), plane wave propagation is assumed.

$$\nabla \times \mu_r^{-1} \nabla \times \overset{v}{E} - k_0^2 \left(\varepsilon_r - j \frac{\sigma}{\omega \varepsilon_0} \right) \overset{v}{E} = 0 \tag{4}$$

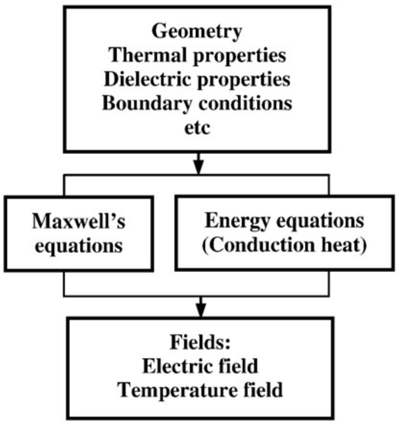

Fig. 4. A schematic model of a paste subjected to microwave energy.

where μ_r is the relative permeability, E^v is the electric field intensity (V/m)), k_0 is the free space wave number, ε_r is the relative permittivity, σ is the electric conductivity (S/m), and ω is the angular frequency (radians per second).

(2) Heat transfer (conduction mode):

4.4. Boundary conditions

4.4.1. Adiabatic boundary condition

Assuming that the surroundings of the paste are insulated (no heat between the system and surroundings):

$$\left. \frac{\partial T}{\partial n} \right|_{sample\,surface} = 0 \tag{5}$$

4.4.2. Continuity boundary condition

For the microwave heating of the cement paste, the temperature and heat flux at the interface of the sample within the microwave cavity to be continuous:

$$T = T', \ \lambda_{\text{eff}} \left. \frac{\partial T}{\partial n} \right|_{\text{boundary}} = \lambda'_{\text{eff}} \left. \frac{\partial T}{\partial n} \right|_{\text{boundary}} \tag{6}$$

4.4.3. Electromagnetic boundary condition

(a) The walls of a cavity are perfect conductors.

$$n \times \vec{E} = 0 \tag{7}$$

where n is the normal vector.

(b) Continuity boundary condition. Boundary conditions along the interface between different materials, air and cement paste, are given by using Ampere's law and Gauss theorem.

$$E_t = E'_t, H_t = H'_t, \varepsilon E_n = \varepsilon' E'_n, \mu H_n = \mu H'_n \tag{8}$$

4.5. Numerical method

A commercial Finite Element package COMSOL™ [14] was employed. A non-uniform triangular grid was in excess of 8.42×10^3 cells, resulting in more than 2.219×10^5 degrees of

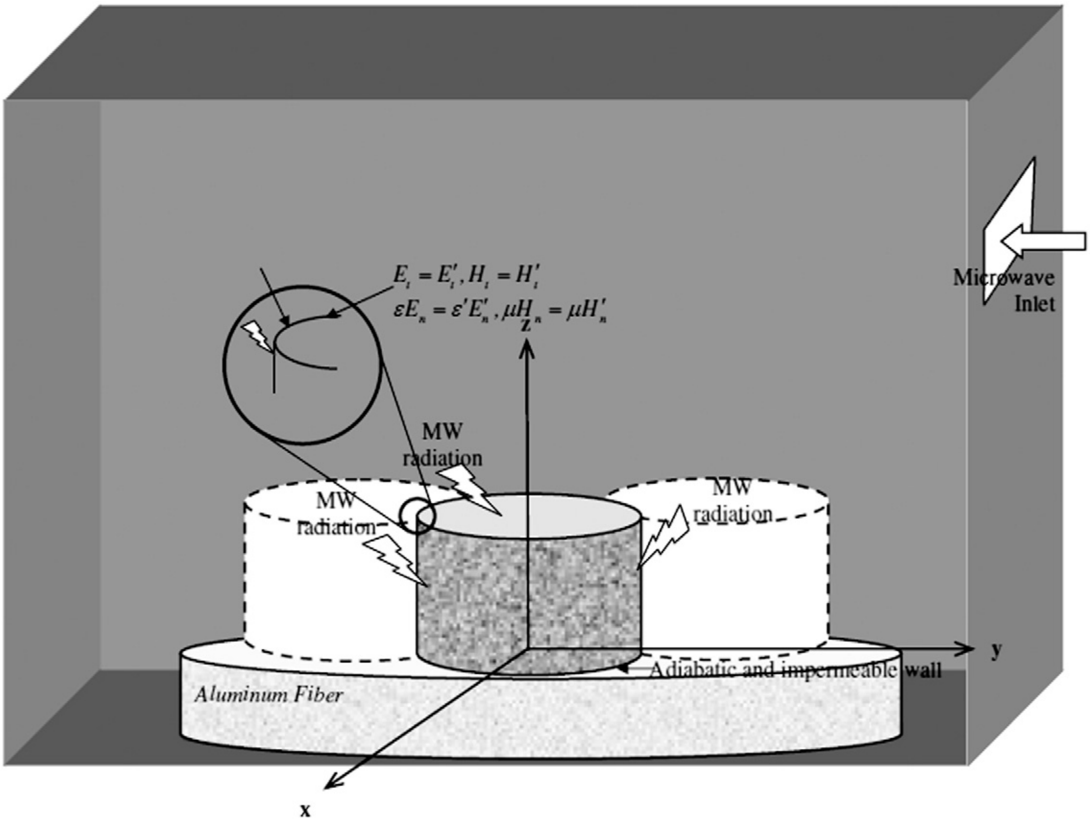

Fig. 5. Physical model.

freedom. The execution time on an Intel® Core™ Quad CPU Q8400@2.66 GHz (3 GB RAM) was 3.02×10^4 s. The tolerance has been kept to 1.0×10^{-3} for all executable variables.

5. Experimental results

5.1. Dielectric properties

Fig. 6 shows the evolution of relative dielectric properties ($\varepsilon'$and ε'') and the simultaneous temperature rise in the cementitious paste. It is observed that during the dormant period, the dielectric property changes very little because the chemical composition of the aqueous paste remains nearly constant [15]. Similarly, relative dielectric properties also appear to be affected by the temperature rise. In the accelerated period of the pastes the highest increasing rate of temperature rises corresponds to the highest decreasing rate of relative dielectric properties.

5.2. Microstructure characteristics

The microstructural characteristics of pastes subjected to microwave energy were investigated by a scanning electron microscope (SEM) with dispersive X-ray (EDX), X-ray diffraction (XRD) and thermal analysis (TG). After mixing and molding, they were cured at room temperature by wrapping with polyethylene plastic until the delay time (time after mixing until introducing microwave energy with a multi-mode cavity) for 30 min. The temperature profile and microwave power of 390 W with a specific application time of 45 min are shown in Fig. 7. The temperatures increase monotonically among the positions of measurement during the microwave curing process and reach a maximum of 105 °C at the bottom surface of the cured cement paste. Significantly, when comparing the obtained temperatures at three positions, the bottom of the cured specimen had highest temperature levels than those of the other sides. It may be due to the fact that during temperature rise, the water at the top side of specimen may be evaporating, so the temperature was dropping gradually, while at the bottom the evaporation of water is difficult. As a result the heat accumulates on the specific side providing a temperature increase with a high rate than the other sides.

A typical micrograph of the paste when subjected to microwave energy is shown in Fig. 8. It is clearly seen that the sample consists of hydrated phases and pores, as well as cores of $Ca(OH)_2$ dendrite crystals or other crystals (marked CH), calcium silicate hydrate (C–S–H), and granular structure. Furthermore, some ettringite (AFt) is founded in the case of specimens cured by microwave energy. It can be described that in the early stages of the reaction of the 27 °C sample, very small (about 1 μm) irregularly-shaped ettringite was formed; but at the same curing time, needle-like ettringite had already formed in 60 °C samples [16,17].

Spectra of various cement pastes with different water-to-cement ratios subjected to normal curing (lime-saturated deionized water) and microwave energy is shown in Fig. 9.

X-ray diffractometry was used to determine the degree of crystallinity of the hydrated cement products and the existence of crystalline coexisting phases. Fig. 10 shows the X-ray patterns of the hydrated products in the paste after applying microwave power of 390 W for 45 min. The phases identified include calcium silicate hydrate (Ca_3SiO_5), calcium hydroxide ($Ca(OH)_2$), residual lime (CaO) and xenotile ($Ca_6(SiO_3)_6(H_2O)$).

The evaluation of the hydration rate in the microwave-cured and normal-cured cement pastes was based on the TG curves. Fig. 11 presents the weight loss that accrues from the water lost in the hydration reactions, the loss of $Ca(OH)_2$ content, and combined loss of

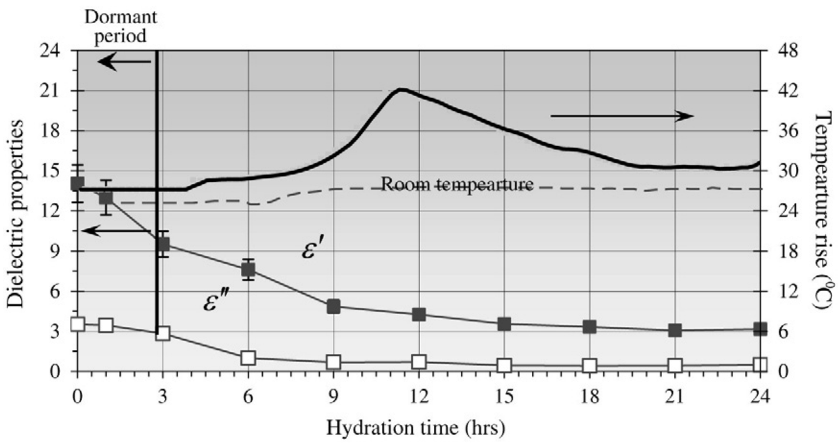

Fig. 6. Dielectric properties.

water and $Ca(OH)_2$ content for the cement pastes when subjected to a microwave energy of 390 W for 45 min. It can be seen that the total water, total $Ca(OH)_2$ content, and water and $Ca(OH)_2$ combined of the microwave-cured cement paste specimen are 10.998%, 2.723%, and 7.243%, respectively. For the $Ca(OH)_2$ content, the 0.38 w/s microwave-cured cement paste is the optimal content for reacting to fully hydrated products, while the higher w/s pastes produce a low concentration of Ca^{2+} and OH^- and consequently crystallize a low Ca $(OH)_2$ content [15].

6. Numerical results and discussion

Based on numerical analysis, the calculated temperature of the paste under microwave exposure times of 5, 15, 30 and 45 min (Table 2) are shown in Fig. 11. It illustrates an increase of the maximum temperature within the samples as the microwave exposure time increases, such that temperatures of 30.21, 59.97, 81.59, and 92.78 °C were reached at exposure times of 5, 15, 30, and 45 min, respectively. In addition, the points at which maximum and minimum temperatures occur are in the middle of the sample. The maximum temperature point arises from the interaction between microwave energy and cement paste.

The predicted and experimental data of the maximum temperature history within the paste when a microwave power of 390 W is applied for 45 min are compared in Fig. 12. The result shows that the predicted data are higher than those of the experimental values. This is mainly due to the fact that the parameter used in this calculation, especially the permittivity value, is kept constant at $\varepsilon_r^* = 15.0861 - j\,4.4458$, while in reality this value decreases continuously as the free water content decreases. That is due to free moisture in paste is transformed to bound moisture [18] resulting in microwave interact with low content moisture owing to low heat generation [15]. In addition, the moisture transfer during microwave heating that affects on the temperature rise is not taken into account in this study. The heat transfer also changes according to how long microwave energy is applied and the formation of hydration products decreases heat transfer with time also. Furthermore, it can be seen that heat generation takes place when the free water can move from the center to another location within the paste; therefore, at the middle point, the temperature is then dropped.

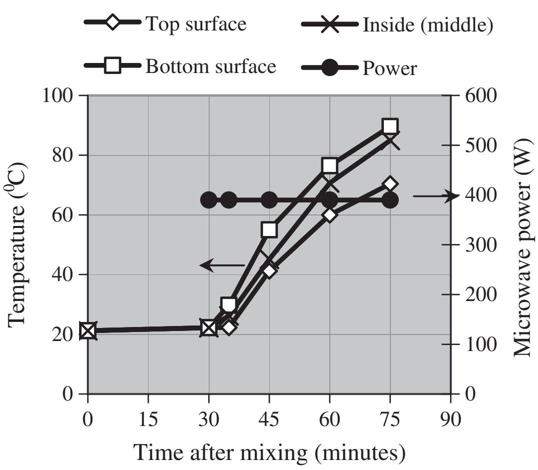

Fig. 7. Temperature and power history during applying microwave energy.

7. Conclusions

The temperature increased monotonically among the positions of measurement during the microwave-curing process. As the micrographs of the microwave-cured paste clearly indicate that the samples consisted of hydrated phases and pores, as well as cores of $Ca(OH)_2$ dendrite crystals or other crystals (marked CH), calcium silicate hydrate (C–S–H), and granular structure. Furthermore, some ettringite (Aft) was found in the specimens cured with microwave energy.

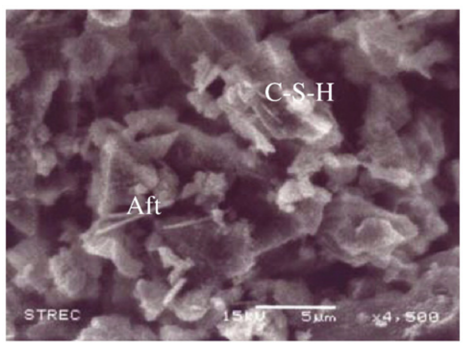

Fig. 8. Micrograph of the microwave-cured paste.

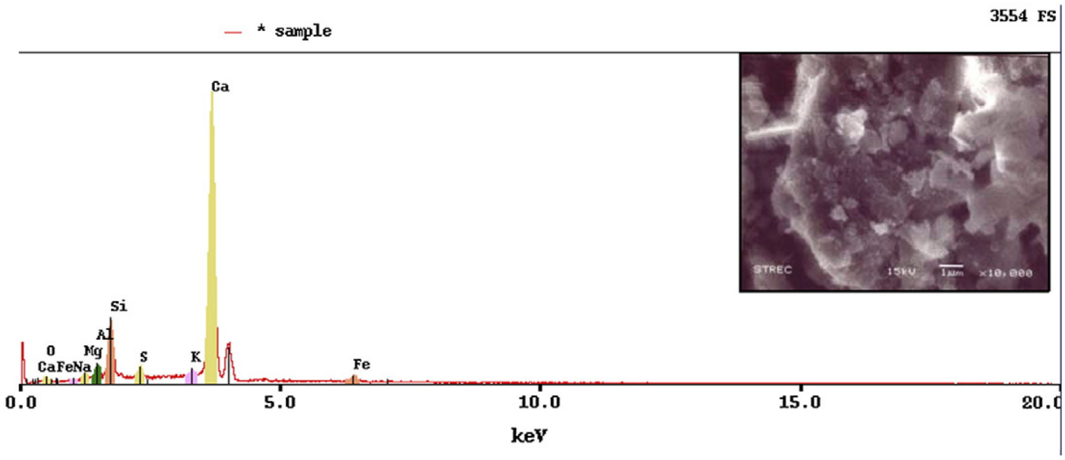

Fig. 9. Spectrums of cement paste after applying microwave energy.

In order to predict the temperature rise during curing by microwave energy, the model explored the interaction between the microwave (electromagnetic field) and cement paste, the heat dissipation (conduction mode) model by using the Multiphysics Modeling and Simulation: COMSOL. The results showed that the simple model associated with assumptions, and initial and boundary conditions can predict the temperature rise higher than those of the experimental data.

Acknowledgments

The authors gratefully acknowledge the Thailand Research Fund (TRF) for supporting this research project.

This paper is dedicated to a great scientist, researcher, philosopher and our guide and colleague Prof. Rustum Roy (July 3, 1924–August 26, 2010), Evan Pugh Professor of the Solid State Emeritus. We will always remember Dr. Roy for his wide ranging intellectual pursuits,

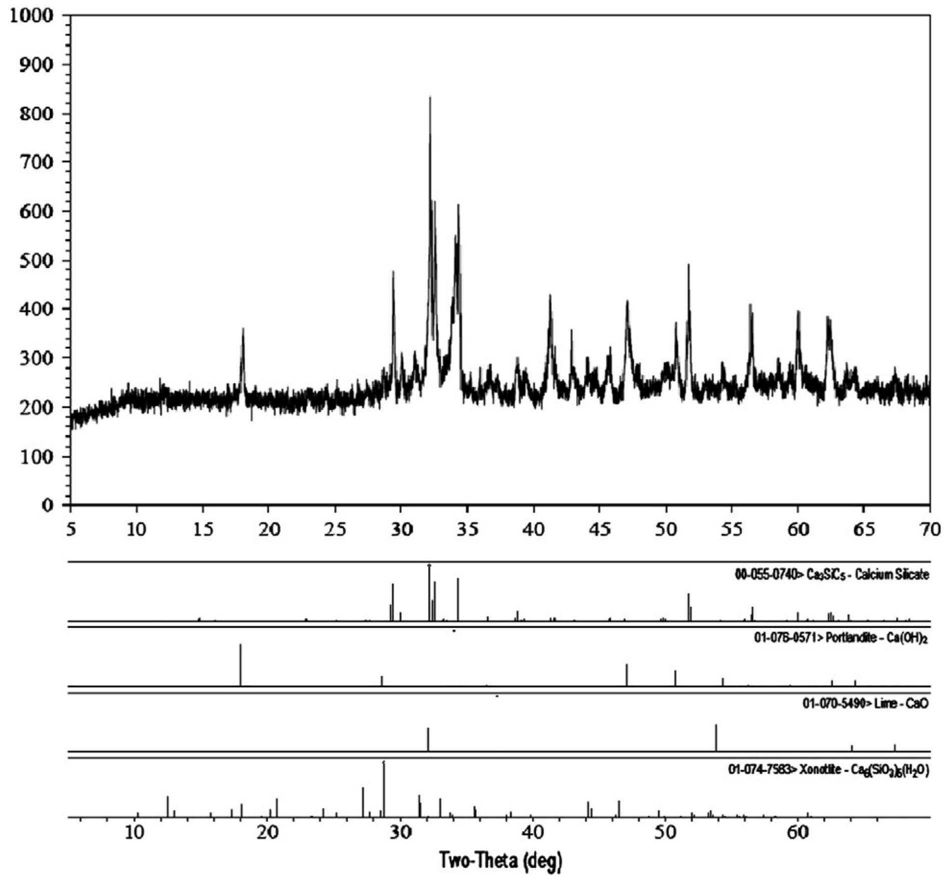

Fig. 10. X-ray diffraction of the pastes after applying MW power 390 W for 45 min, (a) at an application time of 5 min and (b) at an application time of 15 min.

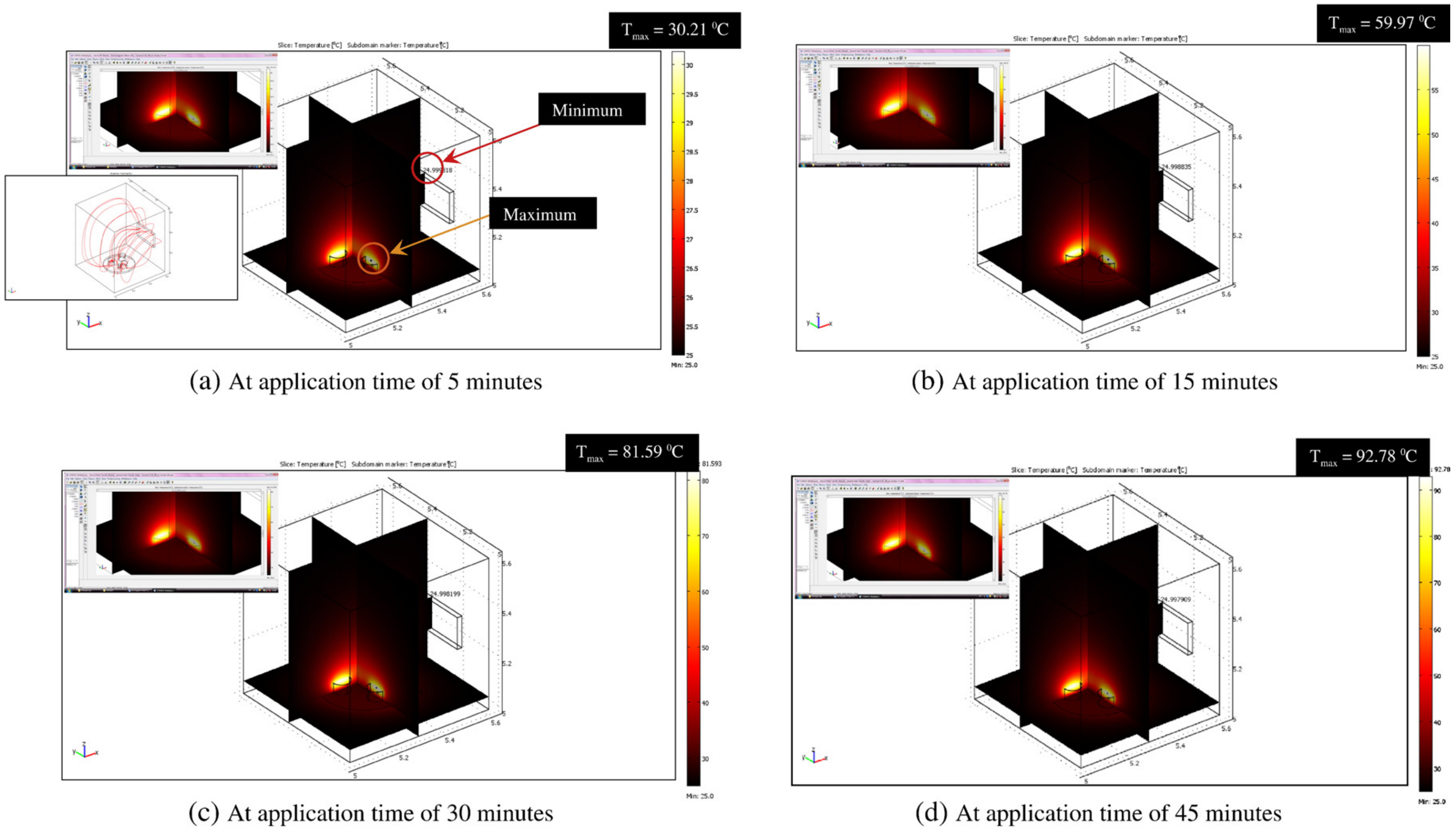

Fig. 11. Temperature distributions of the transient state of 1CW/S_P0.38 paste at times of 5, 15, 30 and 45 min, (c) at an application time of 30 min and (d) at an application time of 45 min. Temperature distributions of the transient state of 1CW/S_P0.38 paste at times of 5, 15, 30 and 45 min.

Table 2
Variables used for calculation.

Variables	Values	Unit	Remark
Scalar			
Sigma_htgh (Stefan–Boltmann constant)	5.67e−0.08	W m^{-2} deg^{-4}	Data bases
Rg_htgh (universal gas constant)	8.31451	J mol^{-1} K^{-1}	Data bases
Epsilon0_rfw (permittivity of vacuum)	8.854187817e−12	F m^{-1}	Data bases
Nu_rfw (frequency)	2.45e9	Hz	Data bases
General heat transfer (htgh)			
Subdomains: air, 1 atm			
k (isotropic)	0.0257	W m^{-1} K^{-1}	Data bases
ρ (density)	1.205	kg m^{-3}	Data bases
C_p (heat capacity at constant pressure)	1.005	J kg^{-1} K^{-1}	Data bases
T (t_0) Initial temperature	293.15	K	Test result
Subdomains: Aluminium 3003-H18			Data bases
k (isotropic)	155	W m^{-1} K^{-1}	Data bases
ρ (density)	2730	kg m^{-3}	Data bases
C_p (heat capacity at constant pressure)	893	J kg^{-1} K^{-1}	Data bases
T (t_0) Initial temperature	293.15	K	Test result
Subdomains: cement paste			
k (isotropic)	$1.005-0.0025\times T$	W m^{-1} K^{-1}	[19]
ρ (density)	1915	kg m^{-3}	Test result
C_p (heat capacity at constant pressure)	$0.75+3.43\times M_f^{water}$ $M_f^{water}=0.38/1.38$	J kg^{-1} K^{-1}	[20]
Q (heat source)	421.0559	W m^{-3}	Test result
T (t_0) Initial temperature	295.35	K	Test result
Boundary condition			
$T=T_0$	298.15	K	Test result
Electromagnetic wave (rfw)			
Subdomains: air, 1 atm			
n (refractive index)	1.0008		Data bases
Subdomains: Aluminium 3003-H18			Data bases
Relative permittivity	1		Data bases
Electrical conductivity	2.326e7	S m^{-1}	Data bases
Relative permeability	1		Data bases
Subdomains: cement paste			Data bases
Relative permittivity	$15.0861-j^{*}4.4458$		At 30 min delay time
Electrical conductivity	1.042	S m^{-1}	Test result
Relative permeability	1		[21]
Boundary condition			
Subdomains: air, 1 atm	Perfect electric conductivity		
Subdomains: Aluminium 3003-H18	Continuity		
Subdomains: cement paste	Port, Power 390	W	
Finite element			
Number of subdomains	7		
Dependent variables	Temperature (T)		
Mesh consists of elements.	84,258	elements	
Analysis type of heat transfer	Steady		
Tolerance	0.01		
Transient duration	5, 15, 30, and 45	min	
Sample	Cement paste		at w/s = 0.38

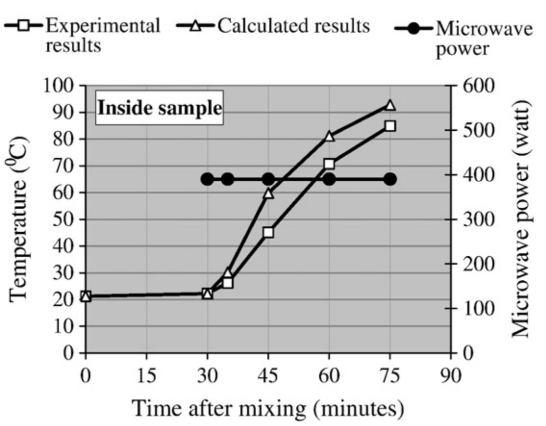

Fig. 12. Temperature history when applying microwave power 390 W on a period of 45 min.

including his pioneering contributions to advance the field of materials science.

References

[1] A.C. Metaxas, Microwave heating, Journal of Microwave Power and Electromagnetic Energy 5 (1991) 237–247.
[2] A.C. Metaxas, R.J. Meredith, Industrial Microwave Heating, Peter Peregrinus, Herts, UK, 1998.
[3] K. Gorur, M.K. Smit, F.H. Wittmann, Microwave study of hydrating cement paste at early age, Cement and Concrete Research 12 (1982) 447–454.
[4] R.H. Haddad, I.L. Al-Qadi, Characterization of Portland cement concrete using electromagnetic waves over the microwave frequencies, Cement and Concrete Research 28 (1998) 1379–1391.
[5] R.G. Hutchison, J.T. Chang, H.M. Jennings, M.E. Brodwin, Thermal acceleration of Portland cement mortars with microwave energy, Cement and Concrete Research 21 (1991) 795–799.
[6] L. Dongxu, W. Xuequan, A study on the application of vacuum microwave composite dewatering technique in concrete engineering, Cement and Concrete Research 24 (1994) 159–164.
[7] W. Xuequan, D. Jianbgo, T. Mingshu, Microwave curing technique in concrete manufacture, Cement and Concrete Research 17 (1987) 205–210.

[8] K.Y.C. Leung, T. Pheeraphan, Microwave curing of Portland cement concrete: experimental results and feasibility for practical applications, Construction and Building Materials 9 (1995) 67–73.
[9] K.Y.C. Leung, T. Pheeraphan, Determination of optimal process for microwave curing of concrete, Cement and Concrete Research 27 (1997) 463–472.
[10] American Society for Testing and Materials, Annual Book of ASTM Standard Vol. 4.01, Philadelphia, PA, USA, 2009.
[11] Hewlet Packar, HP 8510 network analyzer manual, 1995.
[12] Natt Makul, Phadungsak Rattanadecho, Burachat Chatveera, and Dinesh K. Agrawal, Microwave-assisted heating of cementitious materials: relative dielectric properties, mechanical property, and experimental and numerical heat transfer characteristics, International communications in Heat and Mass Transfer (Accepted).
[13] T. Basak, S. Durairaj, Numerical simulation on efficient microwave processing of thermoplastics with ceramic composites, Numerical Heat Transfer; Part A Application 57 (No. 8) (2010) 554–579.
[14] COMSOL©Multiphysics User's Guide, COMSOL AB., Stockholm, 2009.
[15] H.F.W. Taylor, Cement Chemistry, 2nd Ed.Thomas Telford Publishing, Great Britain, 1997.
[16] Scrivener, K.L., Development of the Microstructure during the hydration of Portland cement. Ph.D. Thesis, University of London, 1984.
[17] K.L. Scrivener, The effect of heat treatment of inner product C–S–H, Cement and Concrete Research 22 (1992) 1224–1226.
[18] J. Bendsted, P. Barnes, Structure and Performance of Cement, Spon Press, London, 2002.
[19] K.H. Kim, S.E. Jeon, J.K. Kim, S. Yang, An experimental study on thermal conductivity of concrete, Cement and Concrete Research 33 (2003) 363–371.
[20] P.F. Hansen, J. Hansen, K. Hougaard, E.J. Pedersen, Thermal properties of hardening cement paste, Proceedings of RILEM international conference on concrete at early ages, RILEM, Paris 1982 (1982) 23–36.
[21] H.C. Rhim, O. Buyukozturk, Electromagnetic properties of concrete at microwave frequency range, ACI Materials Journal 95–M25 (1995) 262–271.